JOINT INSTITUTE FOR NUCLEAR RESEARCH

Veksler and Baldin Laboratory of High Energy Physics

Event Shape Variables to study Heavy Ion Collisions at MPD

Final Report of INTEREST Program
Wave 8

February 13th - March 26th, 2023

Dubna, Russia

Submitted by:
Nishant Gaurav
Indian Institute of Science Education and Research Kolkata

Supervisor:
Dr. Ivonne Maldonado
Veksler and Baldin Laboratory of High Energy Physics

Abstract

The investigation of EOS for phase transition of the quark gluon plasma (QGP), which is expected to exist shortly after the big-bang and in the core of neutron stars, motivates the various experimental studies by heavy-ion collisions such as at RHIC-BES and SPS programs. But there is not any conclusive remarks yet. The MPD experiment at JINR allows the exploration of the first order phase transition between QGP and hadronic matter in the region of maximum baryon density at $\sqrt{s} = 4 - 11$ GeV. The formation of QGP during heavy-ions collisions could be indicated by the existence of isotropic outflow of collider products. The collider events of Bi-Bi have been simulated using UrQMD generator at $\sqrt{s} = 9.2$ GeV for 100k events with the impact parameter ranging from 0 to 16 fm, and the results have been analyzed within the ROOT framework. The event shape variables sphericity and spherocity have been studied with the aim to distinguish between the most central from the most peripheral events. The jetty and isotropic event topologies have been analyzed for central, mid-central and peripheral events, and a framework has been built for the further investigation of this phenomenon.

Introduction

In certain regions of the neutron star collision zone, the matter may reach temperatures and baryonic densities of the order so as to give rise the Quark-Gluon Plasma (QGP). Simulations of neutron star collisions are driven by the EOS, which is being investigated in heavy-ion collisions. The model constantly predicts the existence of the first order phase transition between QGP and hadronic matter at large baryon densities. This implies the existence of critical end-point in the diagram (fig[9]). The MPD experiment aims to study the properties of hot and dense nuclear matter, which is believed to exist in the early universe and in the cores of neutron stars (fig[1]). This presents a unique opportunity to study the same phenomenon from two fundamentally different experimental regimes, namely, astrophysics and high energy physics. This would provide us with the useful tools to cross checks for any theoretical understanding of the EOS. The numerous searches have been carried out at RHIC-BES and SPS programs, but there is not any conclusive evidence. At NICA facility, the $\sqrt{s_{NN}}$ range of 4-11 GeV for heavy ion collisions allow to explore the area of maximum baryon density and expected to provide luminosity at least an order magnitude larger than other facilities at similar $\sqrt{s_{NN}}$. Also, the MPD has collider geometry with large and uniform acceptance which changes little with collision energy. This allows to take measurements with reduced systematic uncertainty. In the second stage of operation, this will also provide collisions of polarized protons and deuterons.

This report contains the introduction and discussion of MPD experiment, its componets and the underlying physics goals. The data for the collision events has been generated using UrQMD generator which is based on Monte-Carlo simulation. After briefly discussing about the event shape variables, the experiment results has been analysed using sphericity and spherocity for central, mid-central, and peripheral events for different event topologies ,viz., jetty and isotropic.

The MPD Experiment

The Multi-Purpose Detector (MPD) is a large-scale experimental setup located at the Joint Institute for Nuclear Research (JINR) in Dubna, Russia. The experiment is part of the NICA (Nuclotron-based Ion Collider fAcility) project, which aims to build a new accelerator complex at JINR for heavy-ion collisions. The MPD detector is designed to study the properties of nuclear matter created in collisions of heavy ions in the center-of-mass energy range of 4 to 11 GeV with luminosity of $1 \times 10^{27}\ cm^{-2}s^{-1}$. The experiment is designed to study the behavior of nuclear matter under extreme conditions of high temperature and high density.

Figure 1: Experimental investigation of QGP which exists in the cores of neutron stars.

It aims to investigate the properties of the QGP, a state of matter believed to have existed

shortly after the Big Bang, during the early stages of the universe. The QGP is a hot and dense state of nuclear matter in which quarks and gluons, the constituents of protons and neutrons, are no longer confined within these particles but are instead free to move and interact with one another. By examining the QGP, the MPD experiment intends to shed light on the fundamental nature of matter and the evolution of the universe. It is designed to operate at high collision rates, up to 10,000 collisions per second. It is located on one of the two collider point at racetrack-shaped ring of 503.04m circumference at NICA complex based on Veskler and Baldin Laboratory of High Energy Physics. The Nuclotron accelerates (polarized) protons, (polarized) deuterons as well as heavy ions up to Bi, delivering maximum kinetic energy of 10.71 GeV/u for protons and 3.8 GeV/u for Au ions. Together with LU-20 Linac and specific ion sources, light ions (up to C) is provided to Nuclotron. The beams can be extracted to the Fixed Target Area, where the Baryonic Matter at Nuclotron (BM@N) experiment is operated. The heavy ion beams originate in the KRION source and are first accelerated in the HILac linear accelerator before transferring to the Booster auxiliary accelerator which is the storage of ions with A/Z not larger than 3 and initial acceleration to 600 MeV/u. This allows full stripping of ions during the transfer to Nuclotron. Hence, the Booster and Nuclotron together provide the heavy-ion beams.

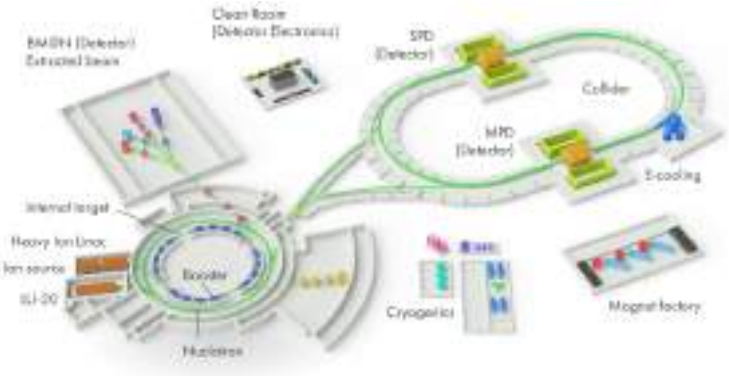

Figure 2: Nica Complex

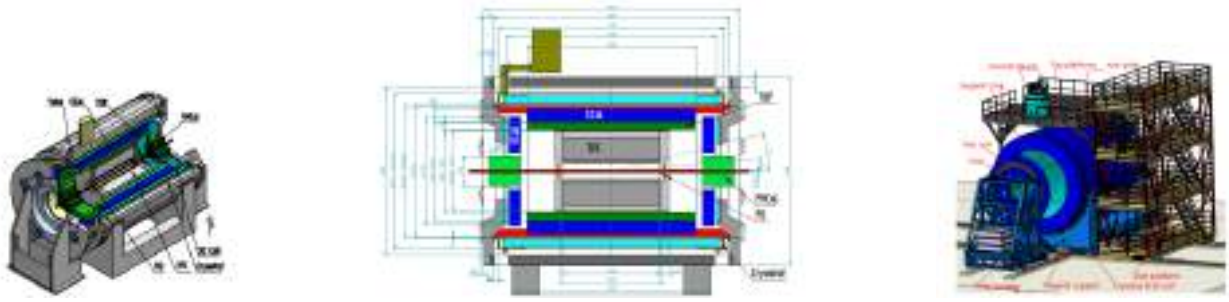

Figure 3: Schematic of MPD Setup

The MPD detector consists of several sub-detectors, each designed to measure different properties of the particles. It is housed in a large, cylindrical magnet that provides the highly homogeneous magnetic fields upto 0.57 T for particle tracking (0.5 T for operational setting by default). It ensures the appropriate transverse momentum resolution for reconstructed particles within the range of momenta of 0.1–3 GeV/c. The sub-detectors are arranged in layers around the collision point, and each layer is designed to measure different types of particles. The sub-detectors include a Time Projection Chamber (TPC), a Time-of-Flight (TOF) system, and an Electromagnetic Calorimeter (ECAL).

The TPC is the main tracking detector of the MPD experiment and is used to measure the trajectory and momentum of charged particles produced in the collisions. It has length of 340 cm with inner and outer radius of 25 cm and 140 cm respectively. It is intended to reconstruct in three dimensions the paths of charged particles produced by the collision. The TPC consists of a large cylinder containing a mixture of argon, methane, and carbon dioxide. When a charged particle passes through a gas, it ionises the atoms of the gas, producing a cloud of electrons that drift towards the endcaps of the chamber. By measuring the arrival time of electrons at the endcaps, it is possible to determine the position of a particle. Hence, it provides 3D tracking of charged particles as well as measurement of specific ionization energy loss for particle identification for $|\eta| < 1.3$.

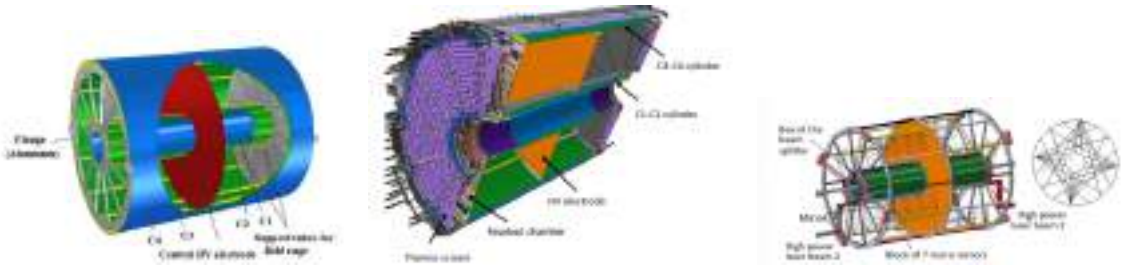

Figure 4: TPC Detector

The TOF system is used to measure the time of flight of charged particles and to identify different particle species based on their velocity, i.e., the TOF detector is utilised to measure the time-of-flight of collision-generated particles, which is a measure of their velocity. The TOF detector is comprised of scintillation counters positioned on both ends of the TPC. When a charged particle passes through the TOF, it generates a brief flash of light that is detected by the scintillation counters. The time difference between the flashes of light produced at the two ends of the TOF is proportional to the velocity of the particle. It is based on Multigap Resistive Plate Chambers (MRPC) detectors and has a total of 28 modules with 13440 channels. It provides the measurement of the particle's arrival time with the time resolution of the order of 50 ps and also measures the position of the track. The TPC-TOF matching allows the particle indentification to distinguish pions from kaons up to 1.5 GeV/c, and protons from pions and kaons up to 2.5 GeV/c.

Figure 5: TOF Detector

The ECAL is used to measure the energy of photons and electrons in heavy-ion collisions. It consits of shashlyk-type towers of approximately 11 interaction lengths with lead absorber and plastic scintillators. It is in the form of cylinder surrounding the TOF, consisting of almost 40,000 towers arranged in projective geometry.

In the forward direction, two detectors are installed:

1. Forward Hadron Calorimeter (FHCal)

2. Fast Forward Detector (FFD)

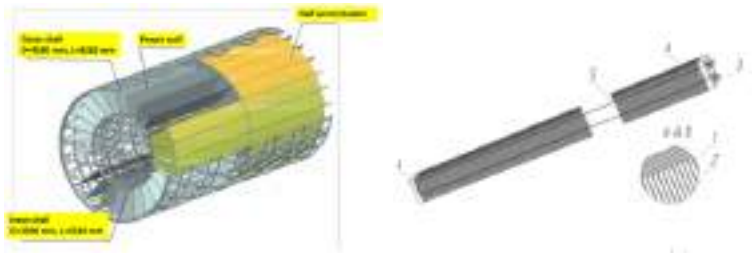

Figure 6: Electro-Magnetic Calorimeter (ECal)

FHCal provides the centrality determination as well as reaction plane measurement. It is composed of 88 modules placed in two parts on the opposite side of the interaction point. Each module consists of 42 lead-scintillator sandwiches read out by WLS fibres. FFD consists of two identical Cherenkov modular arrays FFDE and FFDW with large active area and picosecond time resolution, placed close to the beam pipe. It provides the acceptance region in pseudo-rapidicity of the detector to be in between 2.7 to 4.1, which corresponds to the polar angle of 1.9° to 7.3°. It provides the fast trigerring for nucleus-nucleus collisions, as well as a start time $T_\circ$ for the TOF detector.

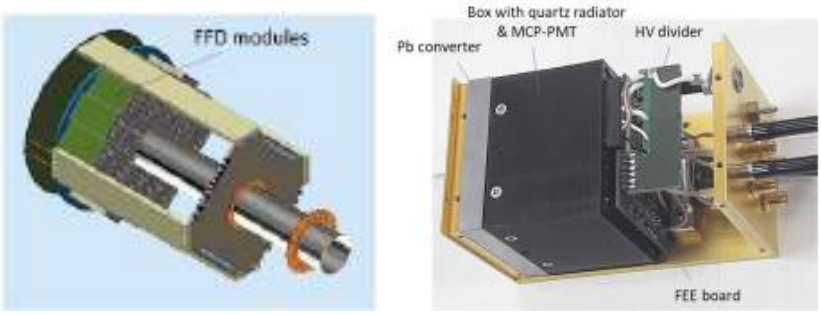

Figure 7: Fast Forward Detector (FFD)

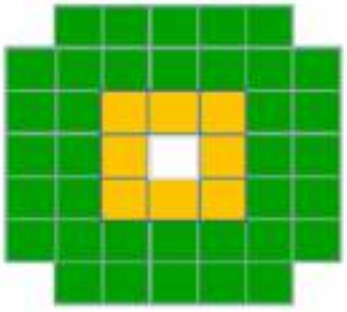

Figure 8: Forward Hadron Calorimeter (FHCal)

SPD is used to measure the position and energy of charged particles that pass through it. It consists of a series of layers of silicon detectors that are used to measure the position and energy of passing charged particles. FCal is used to measure the energy of particles that interact with it and is composed of layers of scintillator material, which are used to measure the kinetic energy of particles that interact with them. In the second stage of MPD construction, silicon-based Inner Tracker system (ITS) will be installed close to the interaction point. This will enhance the tracking and secondary vertex reconstruction capabilities. The miniBeBe detector will be placed between the beam pipe and the TPC, close to the beam. It will aid in triggering and

start time determination for the TOF. Also, the MCORD will be installed on the outside of the MPD Magnet Yoke and it will measure muons flux, and also from the cosmic showers, and is composed of multiple layers of scintillators and tracking chambers.

The physics goals of the MPD experiment include:

- The study of the Equation of State (EoS) of nuclear matter: The EoS describes the relationship between the pressure, temperature, and density of nuclear matter. The MPD experiment aims to study the EoS of nuclear matter in the region of high temperature and high density, which is expected to be reached in heavy-ion collisions.
- The study of the phase transition between hadronic matter and the Quark-Gluon Plasma (QGP): At high temperatures and densities, it is believed that nuclear matter undergoes a phase transition to a state of matter known as the QGP. The MPD experiment aims to study this phase transition and the properties of the QGP.
- The study of collective flow and correlations in heavy-ion collisions: The collective motion of particles in heavy-ion collisions provides information about the initial conditions of the collisions and the properties of the nuclear matter produced. The MPD experiment aims to study the collective flow and correlations of particles produced in heavy-ion collisions.
- The study of strangeness production and hypernuclei: In heavy-ion collisions, it is possible to produce particles containing strange quarks, such as kaons and hyperons.

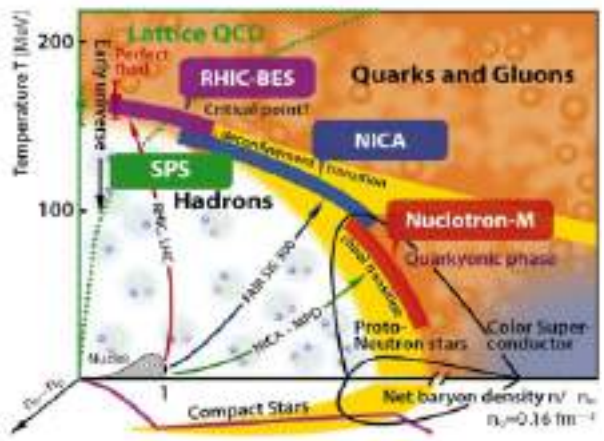

Figure 9: QGP Phase Diagram

The UrQMD Generator

Ultra-relativistic Quantum Molecular Dynamics (UrQMD) generator is a computer programme used to simulate high-energy nuclear collisions. It was created by physicists at the Frankfurt Institute for Advanced Studies in Germany, led by Dr. Marcus Bleicher. Nuclear physicists utilise the UrQMD generator to simulate and analyse the behaviour of nuclear matter under severe conditions, such as those observed in heavy-ion collisions. The UrQMD generator simulates the interactions between particles within a nucleus and between these particles and the surrounding nuclear materials. Using a combination of classical and quantum mechanical techniques, it simulates the dynamics of these interactions in order to provide a comprehensive description of the system's attributes as it evolves over time. The initial conditions of the system, including the type of nuclei, impact parameter, and center-of-mass energy, are specified at the start of the

simulation with a seed for the random number generator. These initial circumstances are chosen to reflect both the qualities of the nuclei colliding and the conditions under which the collision is occurring. The generator then simulates the interactions between the particles, taking into account the numerous forces and processes involved in nuclear collisions, using a number of models and methods. In the present analysis, Bi_{83}^{209} ions of $E_{com} = 9.2$ GeV are colliding with impact parameter ranging from 0 to 16 fm for 100,000 events. Particle list output has happened every 200 fm/c, the calculation has stopped after 200 fm/c. This particular choice allows to compare the results from BES experiment at STAR which collide Au-Au at 9.2 GeV.

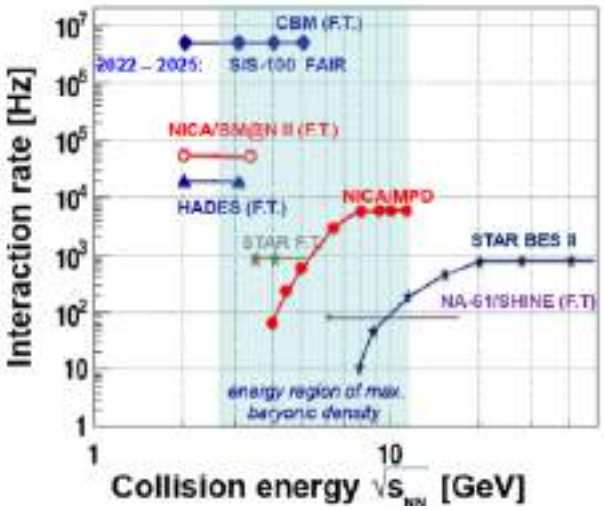

Figure 10: Comparison of energy scale of different experiments to explore QGP physics

The UrQMD generator monitors the trajectories of each particle and the parameters of the system as the simulation progresses. This enables physicists to analyse a vast array of observables, such as the energy distribution of the particles, the momentum distribution, the number and kind of created particles, and the correlation between various observables. The purpose of comparing the findings of UrQMD simulations with experimental data from heavy-ion collision experiments is to validate the models and enhance our understanding of the properties of nuclear matter. The UrQMD generator's capacity to represent the production and decay of resonances and other excited states of the particles involved in the collision is a significant feature. These states can have a substantial effect on the system's overall behavior, and their proper simulation is vital for comprehending the dynamics of nuclear matter under extreme conditions. The generator has been used to investigate a vast array of topics, such as the properties of nuclear matter at high densities and temperatures, the synthesis of quark-gluon plasma, and the production of unusual states of matter, such as hypernuclei.

Event Shape Variables

In high energy physics, event shape variables are quantities used to characterise the shape of particle collisions or events. These variables are computed using the velocities of the particles' final states after a collision. Event shape variables are advantageous because they can be used to distinguish between various types of interactions, to test the Standard Model of particle physics, and to look for new physics beyond the Standard Model.

In high energy physics, there are numerous event shape variables, each with its own unique definition and physical interpretation. Some of the most prevalent event shape variables include:

1. **Sphericity:** Sphericity measures the event's sphericity. It is defined as the minimum ratio of the eigenvalues of the sphericity tensor, which is a matrix constructed from the final state particles' momenta. S=1 corresponds to an event that is perfectly spherical, while S=0 corresponds to an event that is completely flattened along one axis.

2. **Spherocity:** Spherocity is used to characterise the shape of particle collisions. It measures the event's degree of sphericity or non-sphericity. It is defined as the ratio between the minimum and maximum transverse momentum during a collision. It is useful for the study of quark-gluon plasma, a state of matter believed to have existed in the early universe shortly after the Big Bang. It can also be used to differentiate between different types of collisions, such as those involving different types of particles or energies.

3. **Planarity:** Planarity measures the predictability of an event. It is defined as the minimum ratio of the planarity tensor's eigenvalues, which is another matrix constructed from the momenta of the final state particles. P=1 corresponds to an event that is perfectly planar, while P=0 corresponds to an event that is completely three-dimensional.

4. **Aplanarity:** Aplanarity is the complement of planarity and measures the non-predictability of an event. It is expressed as 1-P. A value of A=1 corresponds to an event that is perfectly three-dimensional, while A=0 corresponds to an event that is perfectly planar.

5. **Thrust:** Thrust measures how well an event can be approximated by two jets travelling in opposite directions. It is the maximum ratio of the sum of the momentum of particles on one side of a plane to the total momentum of the event. A value of T=1 corresponds to an event that can be perfectly approximated by two back-to-back jets, while a value of T=0 corresponds to an event that cannot be approximated in this way.

6. **Jet Broadening:** Jet Broadening measures how far apart the jets in an event are from one another. It is the average cosine of the angle between the momentum of each particle and the plane perpendicular to the thrust axis. B=0 corresponds to an event with perfectly back-to-back jets, whereas B=1 corresponds to an event with isotropically distributed jets.

To avoid the bias from the boost along the beam axis at hadron colliders, the event shape variable analyses are restricted to the transverse plane. The transverse momentum matrix is defined as:

$$S^{Q}_{xy} = \frac{1}{\sum_i p_{T_i}} \sum_i \begin{pmatrix} p^2_{x_i} & p_{x_i}p_{y_i} \\ p_{y_i}p_{x_i} & p^2_{y_i} \end{pmatrix} [GeV/c]$$

where p_{x_i}, and p_{y_i} are the transverse momentum projections of the particle i along x- and y-direction respectively, and p_{T_i} is given by $\sqrt{p^2_{x_i} + p^2_{y_i}}$. Since, this quantity is quadratic in particle momenta, implying the sphericity is a non-collinear safe quantity in pQCD. If a parton with high momentum along a transverse plane axis (say x direction) splits into two equal collinear momenta, the sum $\sum_i p^2_{x_i}$ will become half to that of original momentum. The transverse momentum matrix is linearized to avoid this dependence on possible collinear splittings as:

$$S^{L}_{xy} = \frac{1}{\sum_i p_{T_i}} \sum_i \frac{1}{p_{T_i}} \begin{pmatrix} p^2_{x_i} & p_{x_i}p_{y_i} \\ p_{y_i}p_{x_i} & p^2_{y_i} \end{pmatrix}.$$

To define the transverse sphericity the transverse momentum matrix S^{L}_{xy} has to be diagonalized. Let λ_1 and λ_2 be the two eigenvalues with $\lambda_1 > \lambda_2$. The transverse sphericity is then defined as:

$$S_T = \frac{2\lambda_2}{\lambda_1 + \lambda_2}.$$

Another event shape variable named $\mathscr{F}$-parameter is given by

$$\mathscr{F} \equiv \frac{\lambda_2}{\lambda_1}.$$

The transverse spherocity is defined as:

$$S_0 = \frac{\pi^2}{4} \min_{\hat{n}_s} \left(\frac{\sum_i |\vec{p}_{T_i} \times \hat{n}_s|}{\sum_i p_{T_i}} \right)^2$$

where $\hat{n}_s$ is the unit vector which minimizes the above ratio. In a similar way, the transverse thrust τ_T is defined as:

$$\tau_T = 1 - \max_{\hat{n}_\tau} \frac{\sum_i |\vec{p}_{T_i} \cdot \hat{n}_r|}{\sum_i p_{T_i}}$$

where $\hat{n}_r$, also known as thrust axis, is the unit vector which maximizes the sum and hence minimizes the transverse thrust τ_T. Hence it is more sensitive for modelling of two- and three-jet topologies and less sensitive to QCD modelling of large jet multiplicities.

These event shape variables are advantageous because they quantify the shape of high energy particle collisions, which can then be used to test theoretical models and search for physics beyond the Standard Model. They are also essential for comprehending the behaviour of high-energy particle detectors, which rely on measuring the momenta of the final-state particles in order to reconstruct the properties of the collision-produced particles.

Plots

In this section, some of the results obtained from 100,000 collider events of Bi-ions at $\sqrt{s} = 9.2$ GeV have been represented as 1D and 2D histograms of the corresponding kinematic variables and dependence of one quantity on other has also been analysed. The collider data has been generated for events having impact parameter upto 16 fm. In the program developed to analyze the data, the process 1 (abbrv. as pr.1) contains data for all collider events in this case which are being analyzed using ROOT framework. The existence of Protons (including spectators), Kaons, Pions, and Lambda particles can be seen after the collision events and are abbreviated as p, k, pi, la in the plots. The abbreviation ch has been used to represents the charged particles.

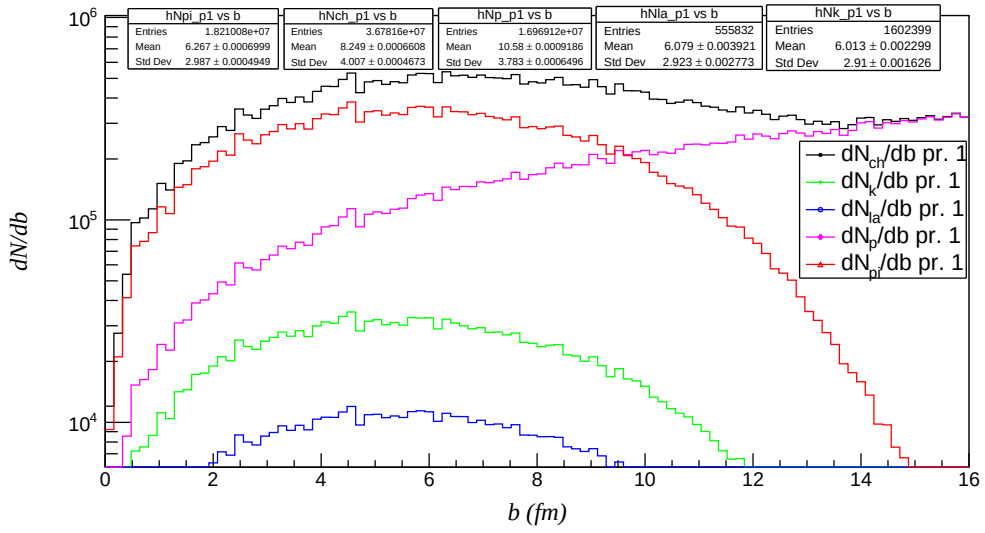

Figure 11: Multiplicity of particles over the impact parameter (b) considered

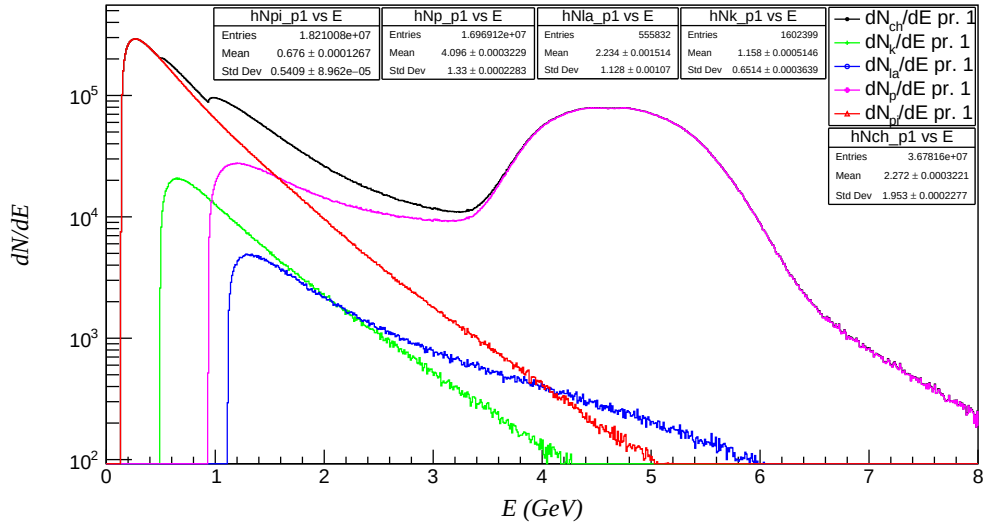

Figure 12: Multiplicity of particles with energy (E)

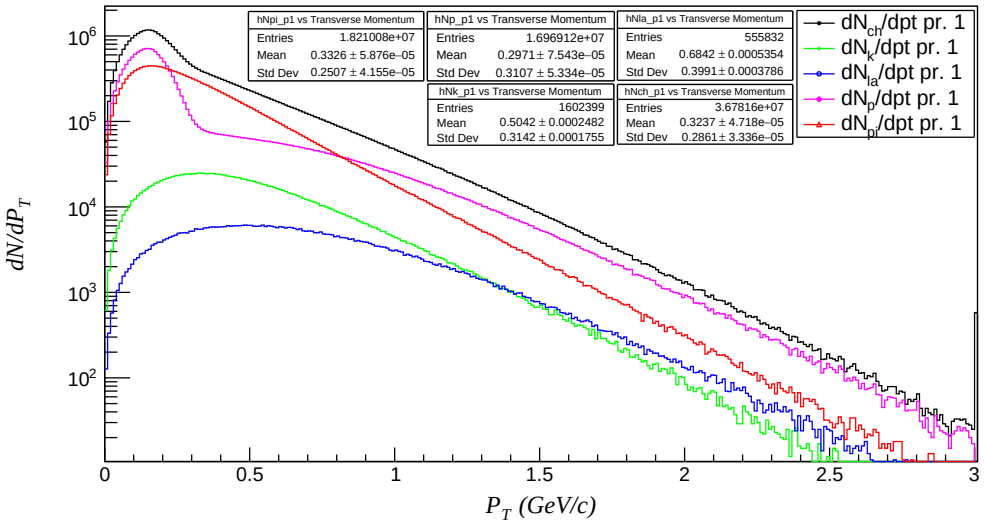

Figure 13: Multiplicity of particles with transverse momentum (P_T)

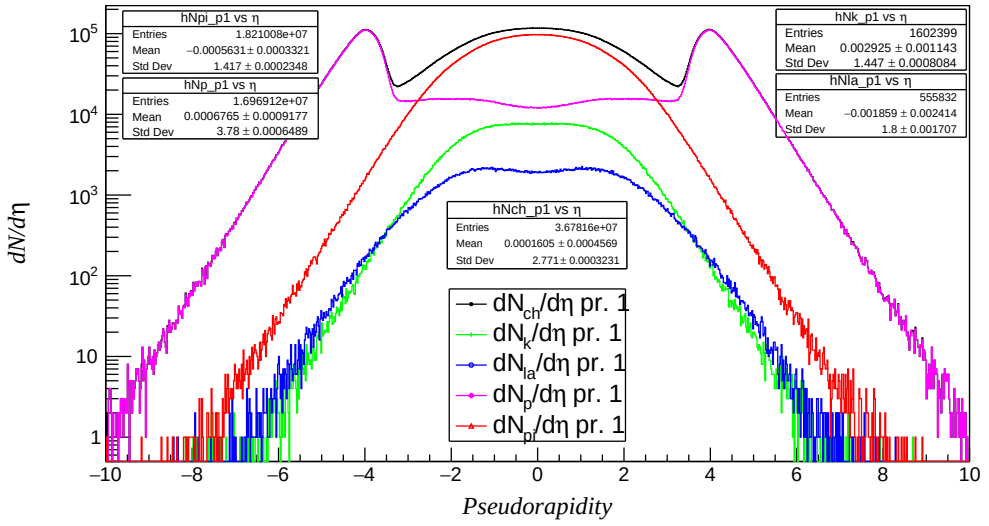

Figure 14: Multiplicity of particles in the given pseudorapidity range

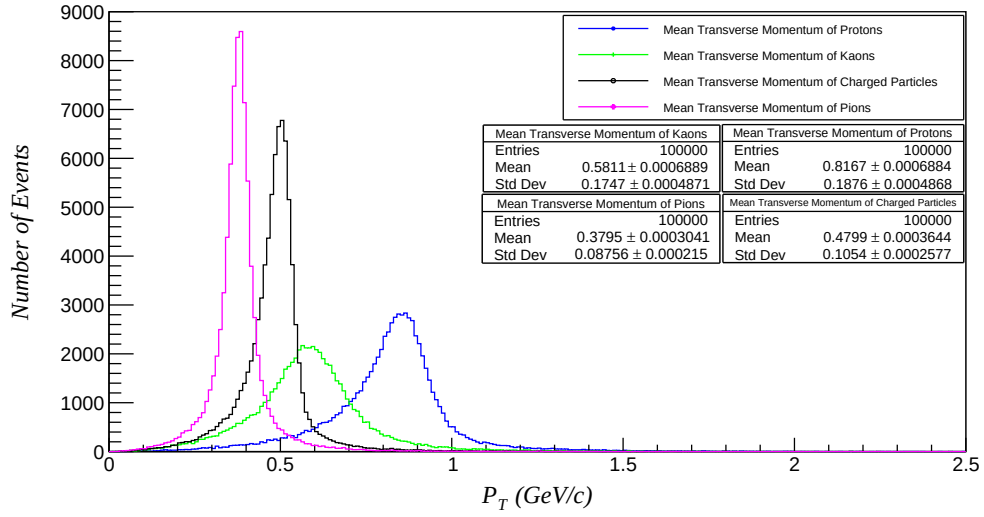

Figure 15: Mean transverse momentum of different particles

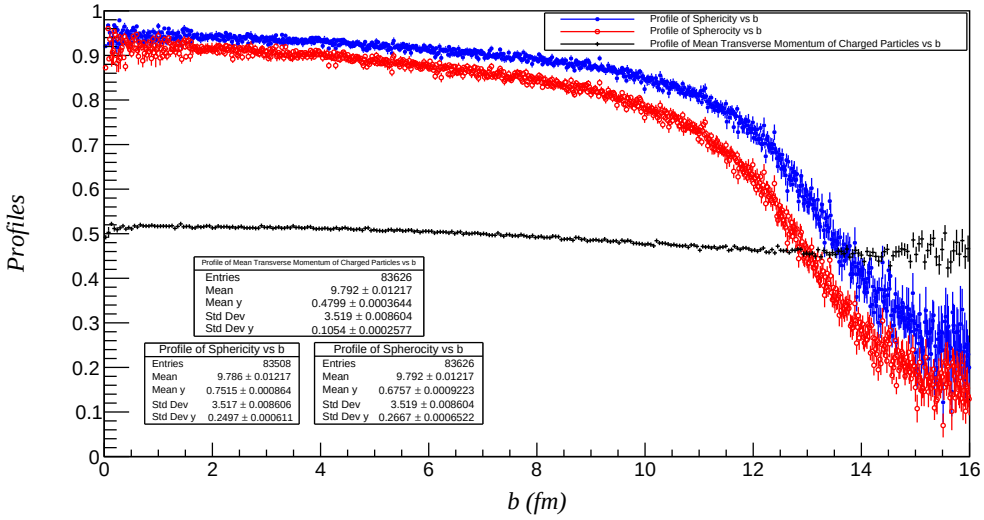

Figure 16: Profiles of Sphericity, Spherocity, and Mean Transverse Momentum for Charged Particles.

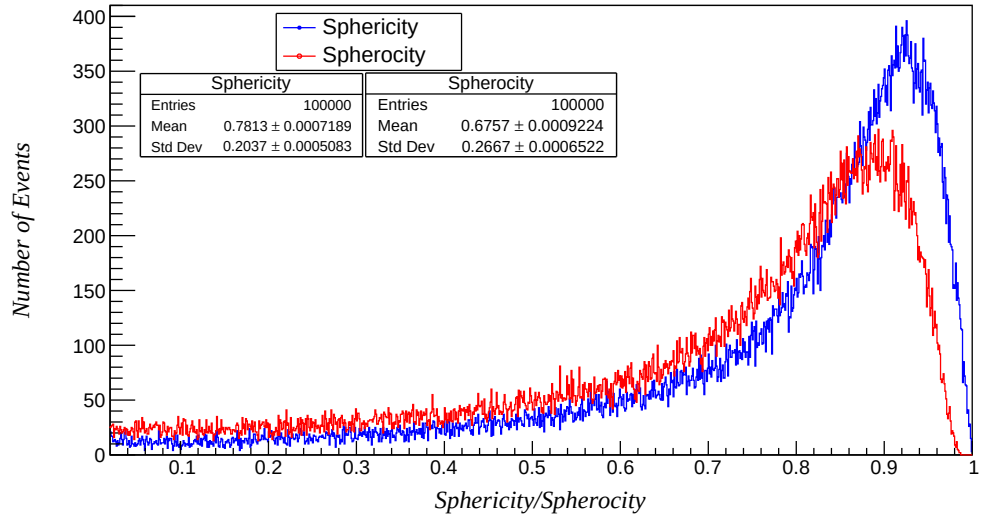

Figure 17: Distribution of sphericity and spherocity with number of events.

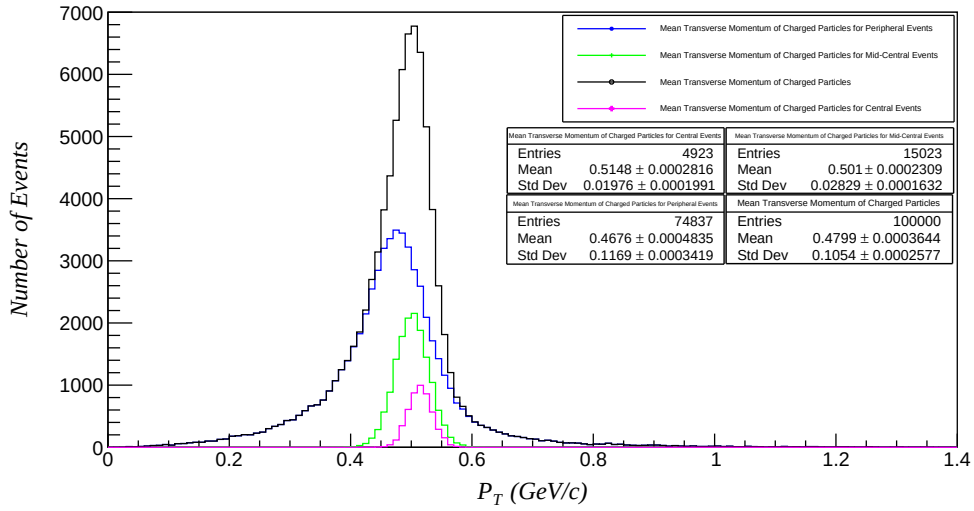

Figure 18: Mean Transverse Momentum of charged particles for different events

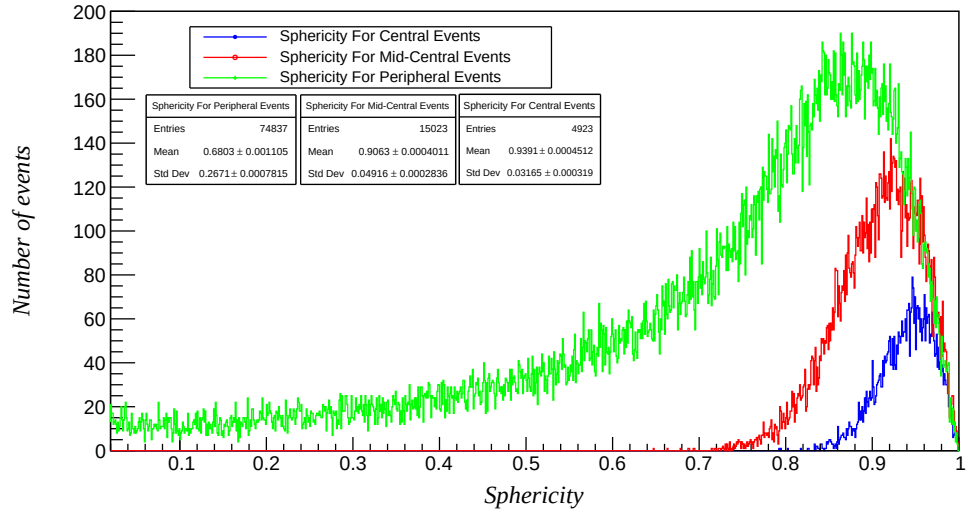

Figure 19: Sphericity of Different Events

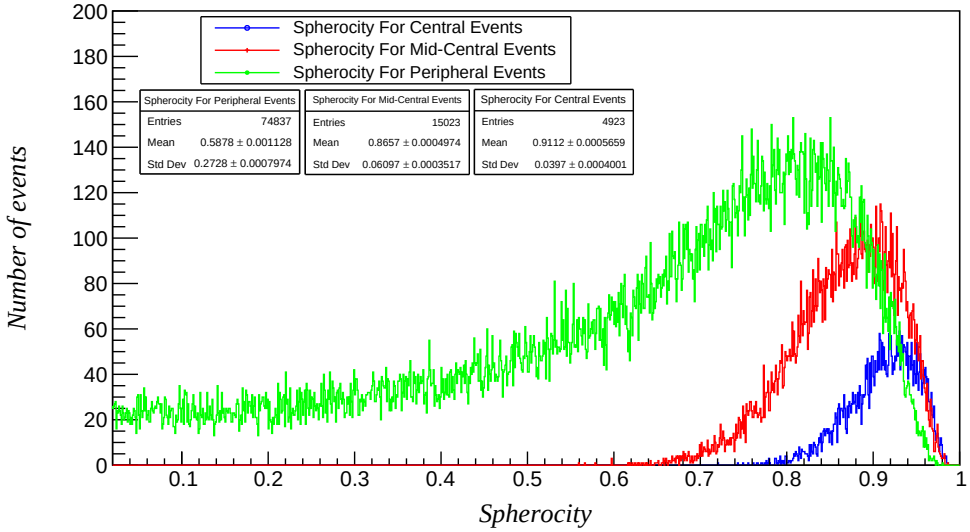

Figure 20: Spherocity of Different Events

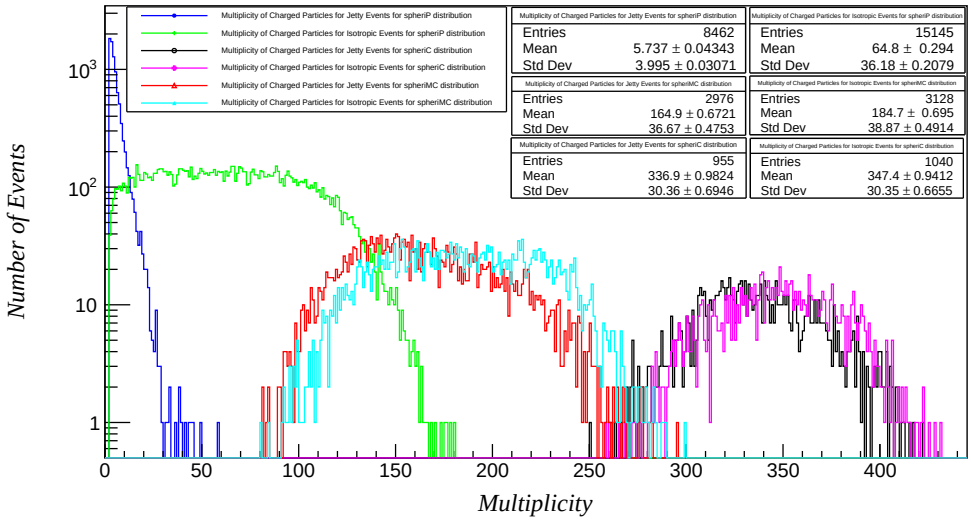

Figure 21: Multiplicity for jetty and isotropic events for spheriP, spheriMC, and spheriP distribution.

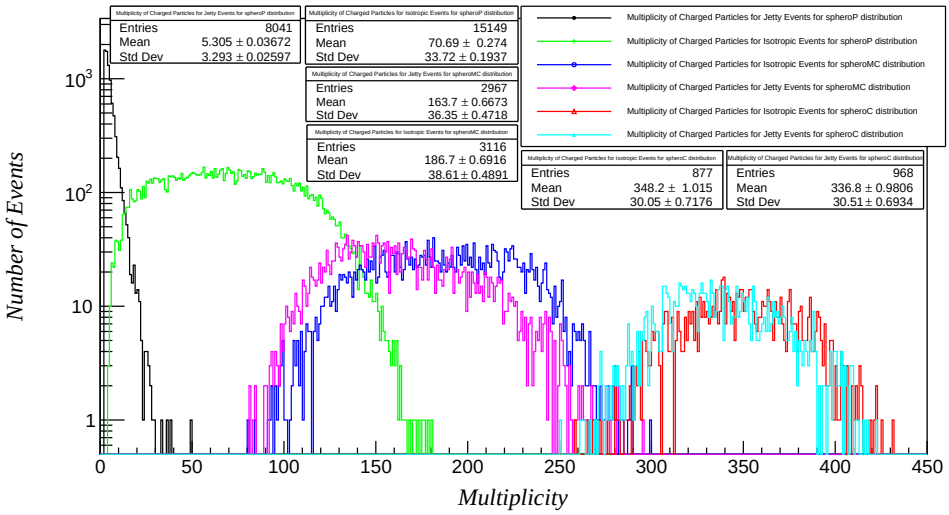

Figure 22: Multiplicity for jetty and isotropic events for spheroP, spheroMC, and spheroP distribution.

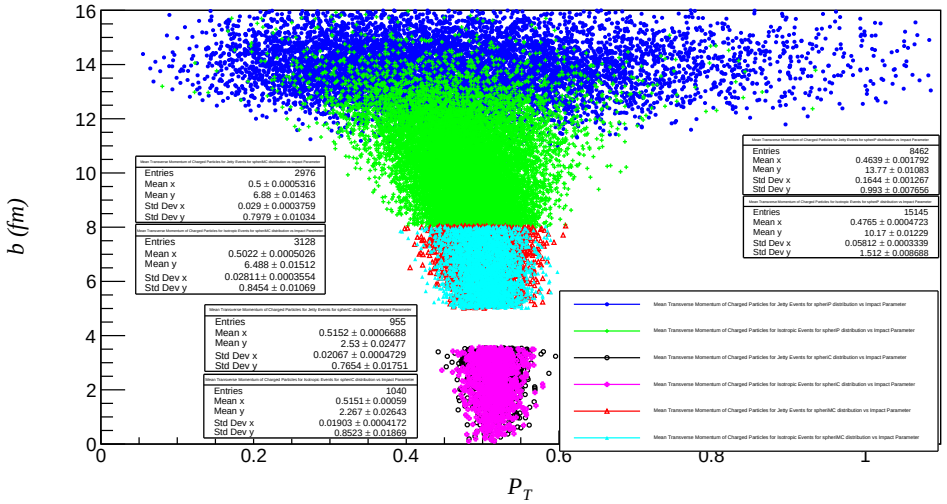

Figure 23: 2D plot of impact paramter vs mean transverse momentum for jetty and isotropic events for spheriP, spheriMC, and spheriP distribution.

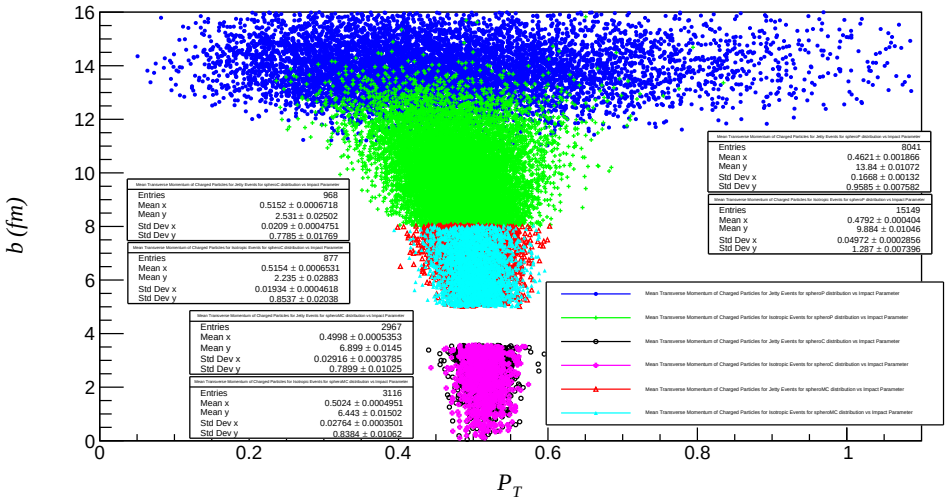

Figure 24: 2D plot of impact paramter vs mean transverse momentum for jetty and isotropic events for spheroP, spheroMC, and spheroP distribution.

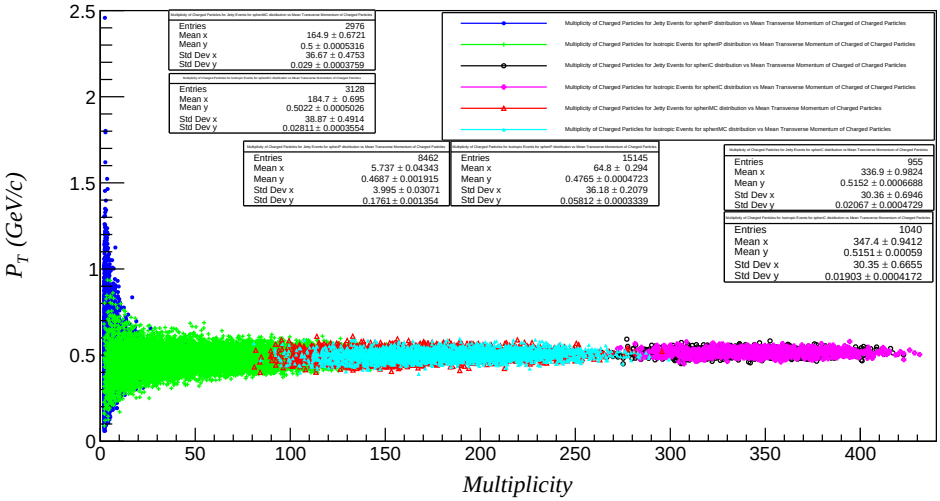

Figure 25: 2D histogram representing the multiplicity for jetty and isotropic events for spheriP, spheriMC, and spheriP distribution against mean transverse momentum (P_T).

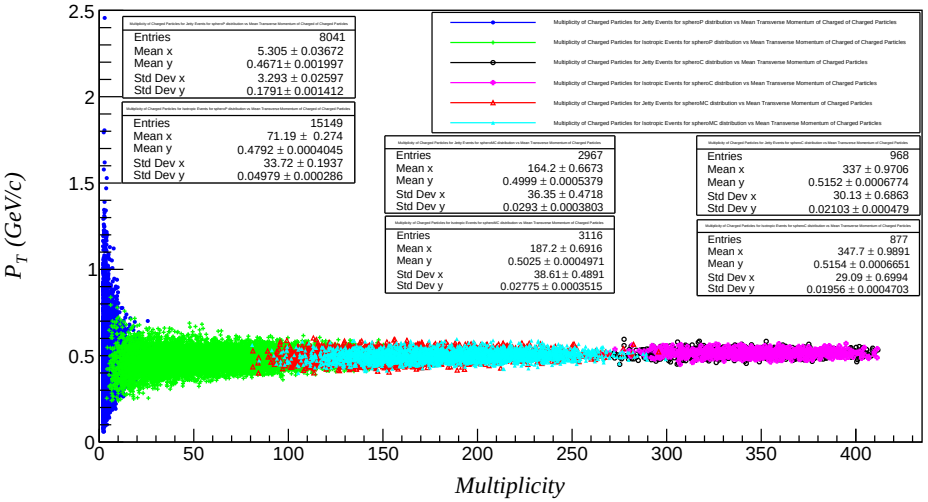

Figure 26: 2D histogram representing the multiplicity for jetty and isotropic events for spheroP, spheroMC, and spheroP distribution against mean transverse momentum (P_T).

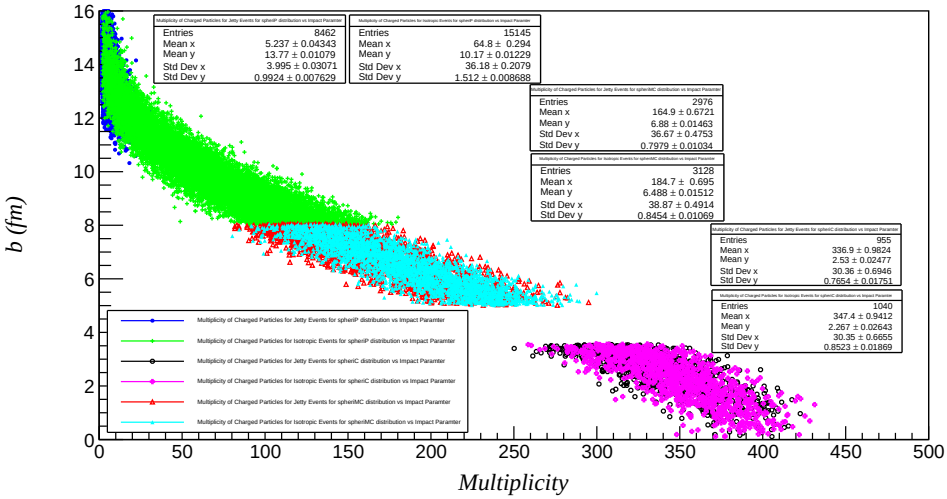

Figure 27: Multiplicity of jetty and isotropic events for spheriC, spheriMC and spheriP distributions against impact paramter (b).

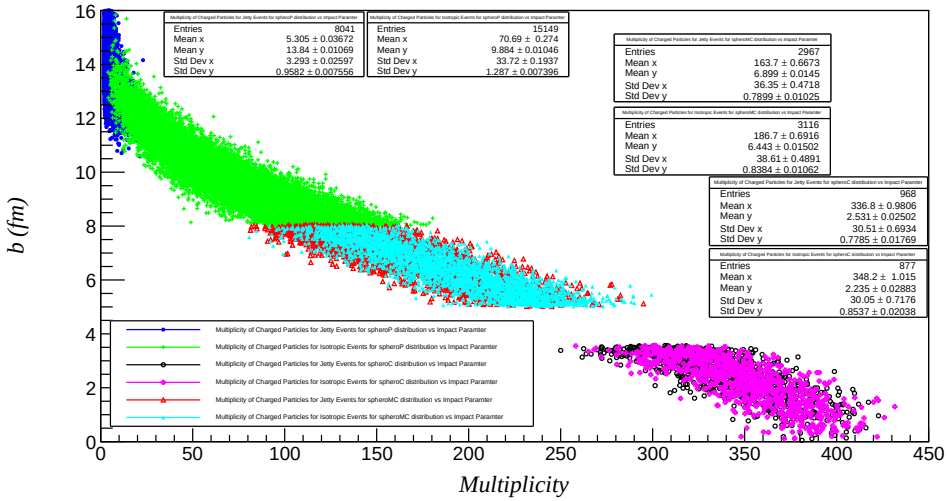

Figure 28: Multiplicity of jetty and isotropic events for spheroC, spheroMC and spheroP distributions against impact paramter (b).

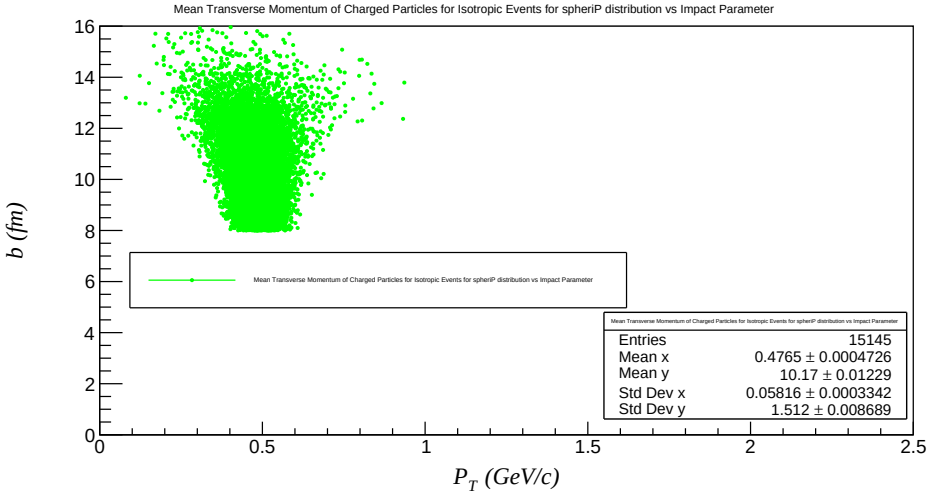

Figure 29: Mean transverse momentum (P_T) of isotropic events for spheriP distribution against impact paramter (b).

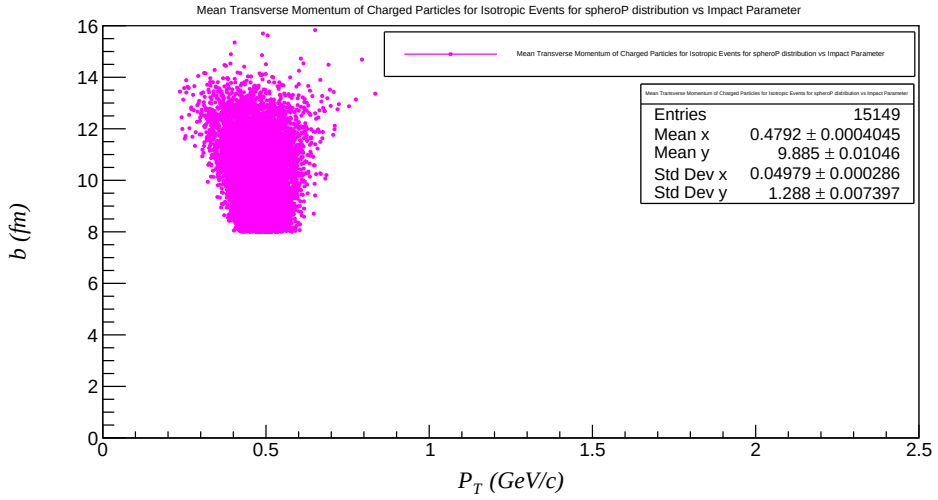

Figure 30: Mean transverse momentum (P_T) of isotropic events for spheroP distribution against impact paramter (b).

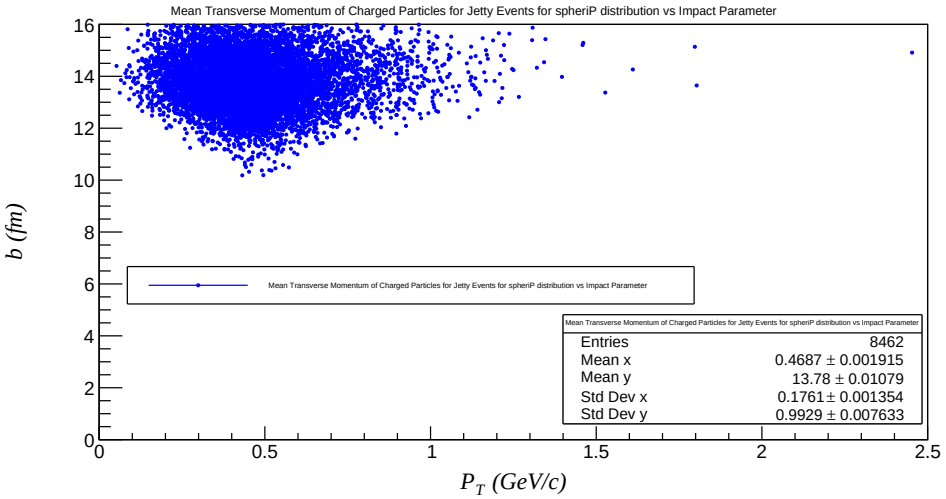

Figure 31: Mean transverse momentum (P_T) of jetty events for spheriP distribution against impact paramter (b).

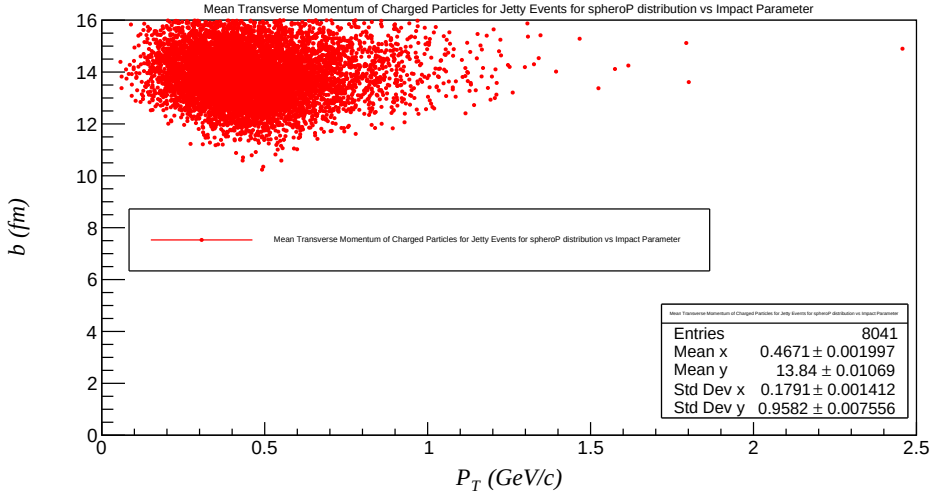

Figure 32: Mean transverse momentum (P_T) of jetty events for spheroP distribution against impact paramter (b).

Results

In our analysis, the focus has been shifted mainly in analysing the charged particles (protons, pions and kaons), and has been studied for different kinematic variables such as energy, transverse momemtum and pseudorapidity. Fig[11] represents the number of particles produced with impact paramter (b). Similarly, fig[12], fig[13], and fig[14] represents the number of particles produced as a function of energy (E), transverse momemtum (P_T), and pseudorapidity (η) respectively. The continous increase in number of protons with impact parameter, a bump in plots of energy and transverse momentum for protons, and peak in the pesudorapidity at approximately +4.4 and -4.4 are indicating the presence of spectator protons. This has been taken care of by implementing the cut in the range of presudorapidity at $|\eta| < 1.3$, which is also the pseudorapidity range of TPC detector. The corresponding mean transverse momentum has been calculated which is shown in fig[15], with mean value of charged particle to be 0.4799 $\pm$ 0.0003644 GeV/c.

The presence of QGP formation in the collider events can be verified from existence of isotropic events, and the most central events are expected to provide the most isotropic events. Based on the centrality, the events have been categorised into central, mid-central, and peripheral events as shown in table[1].

Type of events	**Impact Parameter range (fm)**	**Centrality%**
Central	b$\in$ (0,3.54)	0-10
Mid-Central	b $\in$ (5.04,8.01)	20-50
Peripheral	b$\in$ (8.01,16)	50-100

Table 1: Distribution of central, mid-central, and peripheral events based on impact parameter and centrality

The event shape variables sphericity and spherocity have been used for the present analysis. Fig[16] represents the distribution of sphericity and spherocity with number of events. Fig[15] gives the profile of sphericity, spherocity, and mean transverse momentum with impact parameter. The mean transverse momentum of central, mid-central, and peripheral events have mean value of 0.5148 $\pm$ 0.0002844, 0.501 $\pm$ 0.0002309, and 0.4799 $\pm$ 0.0003644 GeV/c respectively [fig(17)]. Fig(**??**) represent the plot of sphericity and spherocity for different events with following mean values:

Sphericity		
Central	**Mid-central**	**Peripheral**
0.9391 $\pm$ 0.0004512	0.9063 $\pm$ 0.0004011	0.6803 $\pm$ 0.001105

Table 2: Distribution of mean values of sphericity for central, mid-central, and peripheral range for jetty and isotropic events

Spheocity		
Central	**Mid-Central**	**Peripheral**
0.9112 $\pm$ 0.0005659	0.8657 $\pm$ 0.0004974	0.5878 $\pm$ 0.001128

Table 3: Distribution of mean values of spherocity for central, mid-central, and peripheral range for jetty and isotropic events

In the plots, these sphericity ranges for central, mid-central and peripheral events has been abbreviated as speriC, spheriMC, and spheriP respectively. Similar abbreviations has been used in the case of spherocity, i.e., spheroC, spheroMC, and spheroP. From the fig[19, 20], it is quite evident that the sphercity and spherocity value less than 0.65 and 0.6 respectively corresponds to peripheral events. For higher value, there is quite an overlap between central, mid-central and peripheral events. This is implies an need to study these variables using some additional quanties to be able to see clear seperations between different kind s of events. With the aim to study the QGP state, it is also important to differentiate between isotropic and jetty events. Based on first and last 20 % events from central, mid-central and peripheral plots of sphericity and spherocity, the events can be classified into isotropic and jetty for different ranges of sphericity and spherocity as indicated in table[4]. The distribution of multiplities have been shown in fig[21] and fig[22] for sphericity and spherocity respectively. The multiplicity plots for jetty events of peripheral distribution show very distinct behavior and can be differentiated from mid-central and central events. But the isotropic events for peripheral distribution shows the overlap with mid-central distribution along with to that of jetty events of peripheral distribution. A similar observation can be seen in fig[24, 21, 25, 26, 27, 28].

	Sphericity			**Spheocity**		
Events	**Central**	**Mid-central**	**Peripheral**	**Central**	**Mid-Central**	**Peripheral**
Jetty	0-0.912	0-0.877	0-0.871	0-0.912	0-0.815	0-0.335
Isotropic	0.967-1	0.95-1	0.871-1	0.95-1	0.92-1	0.801-1

Table 4: Distribution of sphericity and spherocity range in central, mid-central, and peripheral range for jetty and isotropic events

Although the central and mid-central events have almost overlapped, we will try to see the differences in isotropic and jetty events using the kinematics variables for values of sphericity and spherocity in peripheral range. This has been shown seperately in fig[29, 30, 31, 32] in the 2D histogram plot of impact parameter vs mean transverse momemtum. For jetty events, the mean value for mean transverse momentum for spheriP and spheroP distribution are 0.4687 $\pm$ 0.001915 GeV/c and 0.4671 $\pm$ 0.001997 GeV/c respectively. For isotropic events, they are 0.4765 $\pm$ 0.0004726 GeV/c and 0.4792 $\pm$ 0.0004045 GeV/c respectively. Hence, mean transverse momentum is not a good quantity here for the distinction. From the analysis of mean values of impact parameter, there is higher difference between isotropic and jetty events for spheroP compared to that of spheriP distribution. Although the distinction is not very significant here, and it is difficult to give any remarks.

Conclusion

With the current analysis, events for sphericity and spherocity less than 0.65 and 0.6 respectively can be confidently categorized as peripheral events. Our analysis also showed that indeed, the spherocity is more effective than sphericity in discriminating the multi-jet event topologies. But the current analysis of different event topologies is insufficient in seperating between most central and most peripheral events. I are looking forward for the analysis of more event shape variables, which could be helpful.

Acknowledgement

I am very thankful to JINR Interest Program for providing the suitable platform for carrying out research activities remotely. I want to present my special thanks to Dr. Ivonne Maldonado for her expert guidance and constant support for the entire duration. Her constant availability, regular meetings, and illustrative doubt clearing are the key ingredient which helped in completing the project despite the challenges. I also want to thanks Irving Iván Gaspar Gregorio for the useful discussions which constantly helped me to progress.

Bibliography

[1] V. Abgaryan *et al.* [MPD], "Status and initial physics performance studies of the MPD experiment at NICA," Eur. Phys. J. A **58** (2022) no.7, 140 doi:10.1140/epja/s10050-022-00750-6 [arXiv:2202.08970 [physics.ins-det]].

[2] A. Kisiel [MPD], "Status of the MPD Experiment at JINR," J. Phys. Conf. Ser. **1602** (2020) no.1, 012021 doi:10.1088/1742-6596/1602/1/012021

[3] A. Kisiel, "Overview of the MPD Experiment," Phys. Part. Nucl. **52** (2021) no.4, 501-505 doi:10.1134/S1063779621040328

[4] L. Garren, C. J. Lin, S. Navas, P. Richardson, T. Sjöstrand and T. G. Trippe, "Monte Carlo particle numbering scheme,"

[5] UrQMD User's Guide https://urqmd.org/documentation/urqmd-3.4.pdf

[6] M. Bleicher, E. Zabrodin, C. Spieles, S. A. Bass, C. Ernst, S. Soff, L. Bravina, M. Belkacem, H. Weber and H. Stoecker, *et al.* "Relativistic hadron hadron collisions in the ultrarelativistic quantum molecular dynamics model," J. Phys. G **25** (1999), 1859-1896 doi:10.1088/0954-3899/25/9/308 [arXiv:hep-ph/9909407 [hep-ph]].

[7] H. Petersen, M. Bleicher, S. A. Bass and H. Stocker, "UrQMD v2.3: Changes and Comparisons," [arXiv:0805.0567 [hep-ph]].

[8] Q. Li, Y. Wang, X. Wang, C. Shen and M. Bleicher, "Influence of clustering and hadron potentials on the rapidity distribution of protons from the UrQMD model," [arXiv:1507.06033 [hep-ph]].

[9] S. Cao, "Heavy Flavor Dynamics in Relativistic Heavy-ion Collisions,"

[10] P. Parfenov, I. Selyuzhenkov, A. Taranenko and A. Truttse, "Performance of the MPD Experiment for the Anisotropic Flow Measurement," doi:10.1142/9789811202339_0074

[11] A. Ortiz, "Experimental results on event shapes at hadron colliders," Adv. Ser. Direct. High Energy Phys. **29** (2018), 343-357 doi:10.1142/9789813227767_0016 [arXiv:1705.02056 [hep-ex]].

[12] W. J. Llope, W. Bauer, D. Craig, E. E. Gualtieri, S. Hannuschke, R. A. Lacey, J. Lauret, T. Li, C. M. Mader and A. Nadasen, *et al.* "The sphericity of central heavy-ion reactions," Phys. Rev. C **52** (1995), 1900-1914 doi:10.1103/PhysRevC.52.1900

[13] B. Abelev *et al.* [ALICE], "Transverse sphericity of primary charged particles in minimum bias proton-proton collisions at $\sqrt{s} = 0.9$, 2.76 and 7 TeV," Eur. Phys. J. C **72** (2012), 2124 doi:10.1140/epjc/s10052-012-2124-9 [arXiv:1205.3963 [hep-ex]].

[14] M. Fernández, E. Cuautle and G. Paić, "Event shape variables, a tool for QCD study," J. Phys. Conf. Ser. **761** (2016) no.1, 012031 doi:10.1088/1742-6596/761/1/012031

[15] A. Ortiz, G. Paić and E. Cuautle, "Mid-rapidity charged hadron transverse sphericity in pp collisions simulated with Pythia," Nucl. Phys. A **941** (2015), 78-86 doi:10.1016/j.nuclphysa.2015.05.010 [arXiv:1503.03129 [hep-ph]].

[16] B. Abelev *et al.* [ALICE], "Transverse sphericity of primary charged particles in minimum bias proton-proton collisions at $\sqrt{s} = 0.9$, 2.76 and 7 TeV," Eur. Phys. J. C **72** (2012), 2124 doi:10.1140/epjc/s10052-012-2124-9 [arXiv:1205.3963 [hep-ex]].

[17] A. Banfi, G. P. Salam and G. Zanderighi, "Phenomenology of event shapes at hadron colliders," JHEP **06** (2010), 038 doi:10.1007/JHEP06(2010)038 [arXiv:1001.4082 [hep-ph]].

[18] S. Chatrchyan *et al.* [CMS], "Event Shapes and Azimuthal Correlations in Z + Jets Events in pp Collisions at $\sqrt{s} = 7$ TeV," Phys. Lett. B **722** (2013), 238-261 doi:10.1016/j.physletb.2013.04.025 [arXiv:1301.1646 [hep-ex]].